

1 **Does G_{ST} underestimate genetic differentiation from**
2 **marker data?**

3

4

5

6

J. Wang

7 *Institute of Zoology, Zoological Society of London, London NW1 4RY,*

8

United Kingdom

9

10 *Left running head:* J. Wang

11 *Right running head:* Correlation of G_{ST} and H_S

12 *Key words:* Population Structure, Genetic Differentiation, F_{ST} , G_{ST} , Markers, Drift, Mutations

13 *Corresponding author*

14

15 Jinliang Wang

16 Institute of Zoology

17 Regent's Park

18 London NW1 4RY

19 United Kingdom

20 Tel: 0044 20 74496620

21 Fax: 0044 20 75862870

22 Email: jinliang.wang@ioz.ac.uk

23

24

Abstract

25 The widely applied genetic differentiation statistics F_{ST} and G_{ST} have recently been criticised
26 for underestimating differentiation when applied to highly polymorphic markers such as
27 microsatellites. New statistics claimed to be unaffected by marker polymorphisms have been
28 proposed and advocated to replace the traditional F_{ST} and G_{ST} . This study shows that G_{ST}
29 gives accurate estimates and underestimates of differentiation when demographic factors are
30 more and less important than mutations, respectively. In the former case, all markers,
31 regardless of diversity (H_S), have the same G_{ST} value in expectation and thus give replicated
32 estimates of differentiation. In the latter case, markers of higher H_S have lower G_{ST} values,
33 resulting in a negative, roughly linear correlation between G_{ST} and H_S across loci. I propose
34 that the correlation coefficient between G_{ST} and H_S across loci, r_{GH} , can be used to distinguish
35 the two cases and to detect mutational effects on G_{ST} . A highly negative and significant r_{GH} ,
36 when coupled with highly variable G_{ST} values among loci, would reveal that marker G_{ST}
37 values are affected substantially by mutations and marker diversity, underestimate population
38 differentiation, and are not comparable among studies, species and markers. Simulated and
39 empirical datasets are used to check the power and statistical behaviour, and to demonstrate
40 the usefulness of the correlation analysis.

41

42 Introduction

43 A species rarely breeds at random throughout its whole range to form a homogenous unit.
44 Frequently a species is genetically structured in space, subdivided into subunits called demes,
45 races, subpopulations, ... Delineating the spatial genetic structure by dividing a species into
46 subunits and quantifying the genetic differentiation among the subunits is important in many
47 biological fields such as evolution, conservation, human medicine and forensics. The
48 subdivision can be made based on natural (e.g. rivers) or artificial (e.g. dams or highways)
49 boundaries, on geographical locations, or on genetic data (e.g. Pritchard *et al.* 2000), and the
50 differentiation can be measured from marker data using Wright's (1943) F_{ST} , Nei's (1973)
51 G_{ST} and related statistics such as Weir & Cockerham's (1984) θ and Slatkin's (1995) R_{ST} . The
52 development and wide application of highly polymorphic markers such as microsatellites
53 made these statistics ever more popular, but also caused some confusion and concern. The
54 most popular differentiation statistics, F_{ST} and G_{ST} , are believed to underestimate population
55 differentiation when calculated from markers of high diversity (e.g. Nagylaki 1998; Hedrick

2005; Jost 2008), and for this reason alternative statistics were proposed and advocated to replace them (Hedrick 2005; Jost 2008; Meirmans & Hedrick 2011). The new differentiation statistics, however, are criticized for their lack of biological meaning and applications, their marker dependency but drift independency, and so on (see Ryman & Leimar 2009; Whitlock 2011; Wang 2012).

The claim that F_{ST} and G_{ST} underestimate population differentiation is made from both theoretical and empirical grounds. The mathematical definition of $G_{ST} = (H_T - H_S) / H_T$ suggests that it cannot take values larger than the average within subpopulation homozygosity, $1 - H_S$ (Jin & Chakraborty 1995; Nagylaki 1998; Hedrick 1999, 2005). This constraint is true both mathematically and biologically. Both F_{ST} and G_{ST} are inherently constrained by H_S , as they signify the amount of genetic variation between populations (V_B) as a proportion of the total variation V_T , which is composed of within (V_W) and between (V_B) population variation. A high H_S means a high V_W , and necessarily a low V_B as a proportion of V_T (i.e. low F_{ST} and G_{ST}). However, the constraint imposed on F_{ST} and G_{ST} by H_S does not necessarily mean they are always marker H_S dependent and underestimate differentiation from markers of high H_S , as claimed by some authors (e.g. Nagylaki 1998; Hedrick 1999, 2005; Jost 2008). On the empirical grounds, some studies showed that G_{ST} based on highly polymorphic microsatellites is usually lower than G_{ST} based on weakly polymorphic allozyme loci (e.g. Sanetra & Crozier 2003), and is obviously too low for highly differentiated subspecies (e.g. Balloux *et al.* 2000; Carreras-Carbonell *et al.* 2006). These empirical evidences are true for these particular systems, but do not suggest that F_{ST} and G_{ST} calculated from highly polymorphic markers must always underestimate population differentiation in all circumstances.

Are F_{ST} and G_{ST} dependent on marker diversity? Do they always underestimate population differentiation from markers of high diversity (e.g. microsatellites)? Under which set of conditions do they provide marker dependent (and thus biased) and marker independent (and thus accurate) estimates of population differentiation? Is it possible to detect whether F_{ST} and G_{ST} values calculated from a set of markers underestimate differentiation or not? In this paper, I will use a combination of analytical modelling, simulated data and empirical data to answer these questions. I show G_{ST} is independent of H_S when mutation rate (u) is small relative to migration rate (m) or drift ($1/2N$). Otherwise, G_{ST} decreases nearly linearly with an increase in H_S . The results suggest a test for the presence or absence of mutational effects on G_{ST} . If single-locus G_{ST} values are highly variable and the correlation between single-locus

89 G_{ST} and H_S values is significantly negative, then the observed G_{ST} values are substantially
 90 affected by mutations, are locus specific, and seriously underestimate the differentiation due
 91 to population demography. If the correlation is insignificant, then the observed single-locus
 92 G_{ST} values are unaffected by mutations and are marker independent. They can then be
 93 averaged to give an overall estimate of the genetic differentiation caused by demography only.
 94 Simulations and empirical data are analysed to check the power and statistical properties of
 95 the correlation and regression analyses.

96 **Method**

97 The relationship between G_{ST} and H_S is investigated by analyses of standard population
 98 genetics models of migration, drift and mutation. The results are then verified by analyses of
 99 simulated and empirical datasets.

100 *Theory*

101 Following most previous studies of F_{ST} , I assume a population under the finite island model
 102 of migration (Wright 1931) and the infinite allele model of mutation (Kimura & Crow 1964)
 103 for mathematical tractability. The results and conclusions are, however, applicable
 104 qualitatively to populations under other migration models, such as Wright's (1943) isolation
 105 by distance or neighbourhood model and Kimura & Weiss's (1964) stepping stone model,
 106 and under other mutation models, such as stepwise mutation model for microsatellites or
 107 allozymes (Ohta & Kimura 1973).

108 Under the finite island model with migration rate m among s subpopulations of
 109 effective size N , and under the infinite allele model for a neutral locus with mutation rate u ,
 110 the recurrence equations for the expected homozygosity within a subpopulation, J_0 , and
 111 between two subpopulations, J_1 , is (Nei 1975; Li 1976)

$$112 \quad J_{0(t+1)} = d(a(c + (1 - c)J_{0(t)}) + (1 - a)J_{1(t)}), \quad (1)$$

$$113 \quad J_{1(t+1)} = d(b(c + (1 - c)J_{0(t)}) + (1 - b)J_{1(t)}), \quad (2)$$

114 where $b = m(2 - m)/s$, $a = (1 - m)^2 + b$, $c = 1/(2N)$ and $d = (1 - u)^2$. Equivalently,
 115 J_0 and J_1 are the probabilities that two genes taken at random from within a subpopulation
 116 and from different subpopulations, respectively, are identical in state. The complements, H_S
 117 $= 1 - J_0$ and $H_1 = 1 - J_1$, give the expected (i.e. assuming random union of gametes)

118 heterozygosity or gene diversity (Nei 1973) within and between subpopulations. The total
 119 expected heterozygosity or gene diversity in the entire population is $H_T = (H_S + (s -$
 120 $1)H_1)/s = 1 - J_1 - (J_0 - J_1)/s$ (Nei 1975). Given H_T and H_S , G_{ST} is calculated by $G_{ST} =$
 121 $1 - H_S/H_T$ (Nei 1973). Using (1) and (2), we can calculate recurrently the values of H_S , H_T
 122 and G_{ST} at each generation, given parameters m , N , u , s and initial gene identities $J_{0(0)}$ and
 123 $J_{1(0)}$.

124 Under the joint action of mutation, migration and drift at rates u , m , and $1/(2N)$
 125 respectively, the gene diversity (H_S , H_T) and its distribution (G_{ST}) will reach equilibrium
 126 values. G_{ST} attains its equilibrium value much faster than H_S and H_T , because it is determined
 127 by the strongest (in terms of rate) while H_S and H_T are determined by the weakest among the
 128 forces of mutation, migration and drift. The equilibrium gene identity values are (Nei 1975;
 129 Li 1976)

$$130 \quad J_{0(\infty)} = cd(a - (a - b)d)/G, \quad (3)$$

$$131 \quad J_{1(\infty)} = cdb/G, \quad (4)$$

132 where $G = 1 - d(a(1 - c) + 1 - b) + d^2(a - b)(1 - c)$. The equilibrium gene diversity
 133 and differentiation values, $H_{S(\infty)}$, $H_{T(\infty)}$ and $G_{ST(\infty)}$, can be calculated using (3) and (4). The
 134 expression for $G_{ST(\infty)}$ is complicated, but can be simplified approximately to (Takahata & Nei
 135 1984)

$$136 \quad G_{ST(\infty)} \approx 1/\left[1 + 2N\left(\frac{s}{s-1}\right)\left(\frac{1}{(1-m)^2(1-u)^2} - 1\right)\right]. \quad (5)$$

137 When m , $u \ll 1$, (5) is further simplified to (Takahata & Nei 1984)

$$138 \quad G_{ST(\infty)} \approx 1/\left[1 + 4N\left(\frac{s}{s-1}\right)(m + u)\right]. \quad (6)$$

139 When $s \rightarrow \infty$, (6) again reduces to the equilibrium F_{ST} of the infinite island model of Wright
 140 (1969, page 291), indicating that F_{ST} and G_{ST} are equivalent (Nei 1977; Takahata & Nei
 141 1984).

142 Although several studies have used similar models to investigate the impact of
 143 mutations on F_{ST} and G_{ST} (e.g. Ryman & Leimar 2008; Whitlock 2011), none has examined
 144 the direct relationship between G_{ST} and H_S . Herein I will use equations (1-6) to explore this
 145 relationship in populations in both equilibrium and non-equilibrium conditions under

146 different parameter (m, u, N, s) combinations. This is important as both G_{ST} and H_S are
147 estimable from marker data, and examining the observed patterns of G_{ST} and H_S at a set of
148 marker loci sheds light on the possible impact of mutations on G_{ST} .

149 *Simulations*

150 Simulated data typical of those encountered in practice were generated to test whether the
151 correlation analysis of single locus estimates of G_{ST} and H_S could be used to detect the effect
152 of mutations on G_{ST} when it is present, and whether the analysis does not falsely detect the
153 effect of mutations when it is absent. The behaviour and power of the correlation analysis
154 were investigated by analysing simulated data with varying sampling intensities (of
155 individuals from a subpopulation, of subpopulations, and of markers), different population
156 properties (N, s, m, u) and different mutation and migration models.

157 The simulations considered the finite island model as described above, and a one-
158 dimensional circular stepping stone model (Kimura & Weiss 1964). In the latter model, a
159 number of s subpopulations are arranged in a circle and each subpopulation receives a
160 proportion $m/2$ of its individuals from each of its two neighbouring subpopulations. In both
161 models, each subpopulation is composed of N diploid monoecious individuals. At each
162 discrete generation, the events are mutations, migrations and reproductions occurring in that
163 order. Mutations are assumed to follow either the infinite allele model or the stepwise
164 mutation model. For the former, a mutation always generates a novel allele the population has
165 never seen before. For the latter, the mutated allele increases or decreases in size by 1 repeat
166 with an equal probability of 0.5. For both models, the number of new mutations at a locus in
167 each subpopulation at each generation was sampled from a Poisson distribution with
168 parameter value $2Nu$. For each new mutation, a gene was drawn at random from the $2N$ genes
169 and was changed according to the mutation model. Reproduction is assumed to be random
170 union of gametes, such that selfing and outbreeding occur at rates $1/N$ and $1-1/N$ respectively,
171 and the effective size is equal to the census size for each subpopulation.

172 An ancestral population was assumed to be the same as the subdivided population
173 described above except for population size and structure. It was unsubdivided and had a size
174 $N_A = rsN$, where $r=0.5, 1$ and 2 such that it had equilibrium genetic diversity smaller than,
175 close to, and larger than the subdivided population respectively. The ancestral population was
176 maintained for a large number of generations for it to reach mutation-drift equilibrium at a
177 neutral locus with mutation rate u (which was variable among a number of L loci). It was then

178 subdivided into s subpopulations of size N , which were maintained as described above for g
 179 ($=100, 200, 400$) generations or for a sufficiently large number of generations, in the order of
 180 $\text{Max}(1/u, 1/m, 2N)$, to reach mutation-drift-migration equilibrium. A sample of M individuals
 181 was then taken at random from each of R ($\leq s$) randomly selected subpopulations, and each
 182 sampled individual was genotyped at a number of L loci.

183 The genotype data were then used to calculate Nei & Chesser's (1983) nearly
 184 unbiased estimators of H_S , H_T , and thus G_{ST} ,

$$185 \hat{H}_S = \frac{2\tilde{M}}{(2\tilde{M}-1)R} \sum_{j=1}^R (1 - \sum_{i=1}^k x_{ij}^2),$$

$$186 \hat{H}_T = 1 - \sum_{i=1}^k \left(\frac{1}{R} \sum_{j=1}^R x_{ij} \right)^2 + \frac{\hat{H}_S}{2\tilde{M}R},$$

$$187 \hat{G}_{ST} = 1 - \hat{H}_S / \hat{H}_T,$$

188 where x_{ij} is the frequency of allele i in the sample from subpopulation j , k is the number of
 189 alleles observed in the set of samples from the R subpopulations, and \tilde{M} is the harmonic mean
 190 sample sizes ($\equiv M$ in the simulations).

191 The estimates \hat{H}_S and \hat{G}_{ST} were then used to calculate their correlation coefficient r_{GH}
 192 across loci. The significance of r_{GH} was tested by a permutation analysis in which \hat{H}_S and \hat{G}_{ST}
 193 were both randomized across loci before calculating r_{GH} in 10^6 replicates. The proportion of
 194 replicates in which r_{GH} was smaller than the r_{GH} value calculated from the original data was
 195 taken as the p value. The correlation coefficient was taken as statistically significant when
 196 $p < 0.001$. A significant negative correlation r_{GH} indicates that \hat{G}_{ST} has been affected by
 197 mutations and thus underestimates the differentiation caused purely by demography (drift and
 198 migration). Otherwise, markers with different levels of diversity \hat{H}_S are equally differentiated,
 199 they all give the same G_{ST} expected from the impact of drift and migration only, and the
 200 single locus G_{ST} estimates can be averaged to give a better (in precision) overall estimate of
 201 differentiation.

202 Too many parameter combinations, due to the numerous parameters and the numerous
 203 plausible values of each parameter, are involved in determining \hat{H}_S and \hat{G}_{ST} that a realistic
 204 simulation study can only consider a small fraction of them. I studied the effect of each
 205 parameter in isolation of others each time by varying the values of the focal parameter only
 206 (see Table 1). For each parameter combination, a number of 100 replicate datasets were

207 generated and analysed. The analysis results were reported as the mean correlation coefficient
 208 between \hat{G}_{ST} and \hat{H}_S , \bar{r}_{GH} , and the proportion of replicates with a statistical significant (at
 209 $p < 0.001$) r_{GH} among the 100 replicates.

210 The simulation program was checked by comparing the simulated against the
 211 predicted values of several quantities to make sure it worked properly. First, the effective size
 212 of the entire population in the finite island model is $N_e = sN/(1-F_{ST})$ (Wright 1943; Wang &
 213 Caballero 1999), where F_{ST} can be replaced by G_{ST} . This theoretical prediction was compared
 214 with that estimated from the simulated pedigrees, using the formula $\frac{1}{2N_e} = \frac{\theta_{t+1} - \theta_t}{1 - \theta_t}$ where t the
 215 generation is large and θ_t is the average coancestry at generation t for all individuals in the
 216 entire population. Second, the predicted values of H_S , H_T and G_{ST} by (3-4) were compared
 217 with the corresponding observed values for an equilibrium population under infinite allele
 218 and finite island models. In all situations investigated, the predicted and estimated (observed)
 219 values fitted very well.

220 *Empirical data*

221 The simulation model may be too simple to reflect the reality. In a real population, both m
 222 and N may vary over space and time, and migrations and mutations may not follow the ideal
 223 models assumed in the simulations. Supplementing simulations, therefore, I also analysed
 224 several recently published empirical datasets to demonstrate the use of the proposed
 225 correlation analysis.

226 *Atlantic Salmon*: To investigate the genetic structure of Atlantic salmon populations in the
 227 entire North American range of the species, Moore *et al.* (2014) sampled 9142 individuals
 228 from 153 populations and genotyped each individual at 15 microsatellite loci. They also
 229 sampled 1080 individuals from 50 populations and genotyped each individual at 3192 SNP
 230 loci. The two datasets were analysed separately in the present study of the relationship
 231 between G_{ST} and H_S .

232 *Blacknose sharks*: Using 23 microsatellites and mtDNA sequences, Portnoy *et al.* (2014)
 233 investigated the genetic structure and barriers to gene flow of 10 blacknose shark populations
 234 sampled (651 individuals in total) from the western North Atlantic Ocean. It was found that
 235 the F_{ST} values at the 23 microsatellite loci between the Bahamas and any of the other
 236 populations were more than an order of magnitude greater than the values between any two
 237 of the other populations. Therefore, G_{ST} and H_S values were calculated for each locus in the 2

238 alternative population structures, the 10- and 2-population (Bahamas and the rest) models in
239 the present study.

240 *Mediterranean shore crab*: Schiavina *et al.* (2014) investigated the genetic structure of the
241 Mediterranean shore crab (*Carcinus aestuarii*) in the Adriatic Sea (central Mediterranean),
242 using 11 polymorphic microsatellites in 431 individuals collected from eight sites. One locus,
243 Cae30, has only 5 alleles and a gene diversity of $H_S=0.1$, much lower than the locus with the
244 2nd lowest diversity, which has 13 alleles and a $H_S=0.77$. So Cae30 was excluded as an
245 obvious outlier from the G_{ST} and H_S correlation analysis.

246 *Blacktip reef sharks*: To understand the genetic structure of blacktip reef sharks
247 (*Carcharhinus melanopterus*), Vignaud *et al.* (2014) sampled 758 individuals from 15 sites (4
248 widely separated locations in the Indo-Pacific and 11 islands in French Polynesia) widely
249 distributed in the Indian and Pacific Oceans. Each sampled individual was genotyped at 17
250 microsatellite loci. Three loci (cil169, cli107 and cli12) were found to deviate significantly
251 from Hardy-Weinberg equilibrium and were suspected to contain null alleles (Vignaud *et al.*
252 2014). The three loci were excluded from their original genetic analysis. Herein I investigated
253 the impact of mutations on the estimated differentiation among these shark populations by
254 analysing the relationship between G_{ST} and H_S , using both the entire set of 17 loci and the
255 selected subset of 14 loci.

256 *Copper rockfish*: Using 17 microsatellite DNA loci, Dick *et al.* (2014) assessed the genetic
257 diversity of and the differentiation among ten populations of copper rockfish (*Sebastes*
258 *caurinus*) representing paired samples of outer coast and the heads of inlets in five replicate
259 sounds on the west coast of Vancouver Island, British Columbia. The sample size per
260 population varies between 30 and 105. I calculated the G_{ST} and H_S values at each of the 17
261 loci among the 10 populations, and tested whether the marker differentiation is affected by
262 mutations or not.

263 **Results**

264 *Analytical results*

265 Equation (6) suggests that G_{ST} at neutral loci is determined by the joint action of migration,
266 mutation and drift occurring at rates m , u , and $1/(2N)$ respectively. The relative impact of
267 each evolutionary force on G_{ST} is determined by its rate as a proportion of the total rate,
268 $m+u+1/(2N)$. When subpopulations are small such that drift is the dominating force (i.e.

269 $1/(2N) \gg u+m$), then $H_S \rightarrow 0$ (i.e. fixation) and $G_{ST(\infty)} \rightarrow 1$ in equilibrium conditions. When
 270 mutation is weak relative to drift and migration (i.e. $u \ll 1/(2N) + m$), then $G_{ST(\infty)} \approx$
 271 $1 / \left[1 + 4N \left(\frac{s}{s-1} \right) m \right]$, which suggests that $G_{ST(\infty)}$ reflects demography only and all loci with
 272 varying but small u have the same expected G_{ST} . In contrast, for loci with a high u in a
 273 population with a large N and a small m (i.e. $u \gg 1/(2N) + m$), $G_{ST(\infty)}$ becomes locus (or
 274 mutation) dependent and covaries with locus specific H_S (below). In such a case, marker
 275 based $G_{ST(\infty)}$ has little bearing on population demography, the $G_{ST(\infty)}$ value calculated from
 276 one set of loci can hardly be congruent with that from another set of loci, and it is
 277 incomparable among studies, species and loci.

278 Figure 1 plots the equilibrium G_{ST} as a function of H_S , calculated by (5) and (3)
 279 respectively, for different parameter combinations of u , m and N , assuming $s=10$. When
 280 differentiation is expected to be small due to either strong migration ($m \geq 0.01$) or weak drift
 281 ($N \geq 2500$), G_{ST} keeps constant and does not vary with H_S in its entire range of $[0, 1]$ caused by
 282 widely varying u values in range of $[10^{-6}, 10^{-2}]$. The observation disproves the belief that G_{ST}
 283 underestimates differentiation and becomes H_S dependent when H_S is high (e.g. Nagylaki
 284 1998; Hedrick 1999, 2005; Jost 2008). High H_S values (say 0.95) do constrain G_{ST} to small
 285 values with a maximum of $1 - H_S$, but do not necessarily lead to underestimated and locus-
 286 varying G_{ST} . What is relevant is the main mechanism (determined by the relative strengths of
 287 mutation, drift and migration) leading to the observed high H_S , not the observed high H_S *per*
 288 *se*. A high H_S is usually due to a high u or/and a high N . However, as long as m is much
 289 higher than u , G_{ST} is virtually independent of H_S .

290 When drift is strong (i.e. N small) and migration is weak relative to mutations, G_{ST}
 291 decreases almost linearly with an increasing H_S due to an increasing u (Figure 1). Only in this
 292 situation is the belief that G_{ST} covaries with H_S (e.g. Nagylaki 1998; Hedrick 1999, 2005; Jost
 293 2008) certified. For the parameter combination $N=250$, $m=0.001$, and $s=10$ in Figure 1, for
 294 example, G_{ST} keeps almost a constant value of 0.45 when u varies between 10^{-6} and 3×10^{-6}
 295 that leads to a H_S varying between 0 and 0.5. With $u > 3 \times 10^{-6}$ and thus $H_S > 0.5$, G_{ST} begins to
 296 decrease linearly with an increasing H_S (or u). Similar results are obtained with other values
 297 of the number of subpopulations (s).

298 Many generations, in the order of $1/m$, $1/u$ or $2N$ whichever is the smallest, are
 299 required for a subdivided population to reach the equilibrium differentiation. Natural

300 populations may never reach such equilibrium as m and N are constantly changing. It is thus
 301 important to check whether the above observations (Figure 1) also apply to non-equilibrium
 302 populations. Figure 2 plots G_{ST} as a function of H_S at generations 50, 200 and 1000 since the
 303 subdivision. Mutation rate (u) is assumed to vary from 10^{-6} to 10^{-2} , and the initial gene
 304 diversity is assumed to be $J_{0(0)} = J_{1(0)}$ and to take values $rJ_{0(\infty)}$, where $r=1, 0.5$ and 0.25 . The
 305 relationship between G_{ST} and H_S in a non-equilibrium population is similar to that in an
 306 equilibrium population (Figure 1). Whenever $u \ll 1/(2N) + m$, G_{ST} does not vary with H_S (or
 307 u). Depending on u as well as N and m , H_S can freely vary in almost the entire range of $[0,1]$
 308 without affecting the value of G_{ST} . Otherwise, G_{ST} decreases nearly linearly with an
 309 increasing H_S (or u). The further away a population departs from the equilibrium, the less
 310 affected it is by mutations because the latter require time to accumulate. When $N=250$, for
 311 example, mutations start to have a substantial impact on G_{ST} at generations 50, 200 and 1000
 312 when $H_S \geq 0.8$ ($u \geq 0.0015$), $H_S \geq 0.5$ ($u \geq 0.00001$) and $H_S \geq 0.3$ ($u \geq 0.00003$) respectively.
 313 Initial gene identities (or diversities) seem to have little effect on the relationship between G_{ST}
 314 and H_S at any generation.

315 *Simulation results*

316 Confirming the analytical results presented above, simulations show that, when mutations are
 317 strong relative to migrations ($m=0.001$), G_{ST} estimates vary among loci that have different u
 318 and thus different H_S , and are negatively correlated with H_S (Figure 3). This is true for the
 319 finite island and stepping stone migration models, and for the infinite allele, finite allele and
 320 stepwise mutation models. This is also true no matter the population is at mutation-drift-
 321 migration equilibrium (Figure 3) or not (data not shown). The negative correlation in stepping
 322 stone migration model and infinite allele mutation model is stronger than that in other
 323 migration and mutation models. In contrast, when mutations are weak relative to migrations
 324 ($m=0.01$), G_{ST} estimates are small and are almost constant among loci with different u and
 325 thus different H_S . This is shown for an equilibrium population under different migration and
 326 mutation models (Figure 3), but is also true for non-equilibrium populations (data not shown).

327 When migrations are weak relative to mutations such that G_{ST} is substantially affected
 328 by u and becomes negatively correlated with H_S , a modest sampling effort is needed to detect
 329 the correlation for different migration and mutation models (Figure 4). This is also true for
 330 populations that have not reached mutation-drift-migration equilibrium (data not shown).
 331 Setting the statistical significance at a conservative level of $p < 0.001$, the false detection rate

332 of mutational effects is low (generally below 7%), while the power is generally above 60%
 333 except when less than 10 loci and less than 4 subpopulations are used in the analysis. In
 334 agreement with the results in Figure 3, the correlation analysis is less powerful for the island
 335 migration model coupled with the stepwise or 2-allele mutation model than other models.
 336 While the power increases with the numbers of sampled loci and sampled subpopulations
 337 (Figure 4), it is little affected by the number of sampled individuals per subpopulation, M , as
 338 long as $M > 10$. This is not surprising because the population is highly differentiated for the
 339 parameter combinations and just a few individuals per subpopulation would allow for a good
 340 estimate of G_{ST} .

341 *Empirical analysis*

342 The Atlantic salmon data clearly show an extremely strong negative correlation ($r = -0.953$)
 343 between G_{ST} and H_S estimates among the 15 microsatellites (Figure 5A), with a p value of
 344 0.0×10^{-6} . These markers are highly polymorphic, with H_S varying between 0.66 and 0.94 and
 345 with the number of observed alleles varying between 15 and 91. Compatible with a
 346 substantial impact of mutations, these markers have low but highly variable G_{ST} values,
 347 varying between 0.02 and 0.09 with a mean of 0.045 and a coefficient of variation of 0.629.
 348 These single locus G_{ST} values are all highly significant, as determined by permutation
 349 (permuting individuals among subpopulations) tests.

350 In contrast, the correlation between G_{ST} and H_S estimates of the 3192 SNPs (Figure
 351 5B) is positive and small ($r = 0.044$), with a p value of 0.993 which is insignificant. H_S values
 352 distribute nearly uniformly in the range [0, 0.5]. While most SNPs have G_{ST} values of about
 353 0.1, quite a few outliers show G_{ST} values well above 0.4. The mean G_{ST} is 0.099 for the 3192
 354 SNPs and is 0.091 when the outlier SNPs with $G_{ST} > 0.3$ are removed. Both values are much
 355 larger than the mean G_{ST} across the 15 microsatellites which is 0.045. The comparison
 356 between SNPs and microsatellites further verifies that the differentiation at microsatellites is
 357 greatly impacted by mutations and thus underestimates the underlying population
 358 differentiation due to demography.

359 The blacknose sharks have highly variable single-locus G_{ST} values, with the highest
 360 being 0.35 and 0.18 and the lowest being 0 and 0 for the 2- and 10-population models
 361 respectively (Figure 5C). Among the 23 microsatellites, G_{ST} and H_S estimates are moderately
 362 negatively correlated, with a correlation coefficient of -0.41 ($p = 0.017$) and -0.43 ($p = 0.007$)
 363 for the 2- and 10-population models respectively. None of the correlations are significant at

364 $p=0.001$, but there is a clear trend of less differentiation at more polymorphic marker loci
365 which indicates that mutations might have reduced the G_{ST} values at these loci.

366 The differentiation calculated from each of the 10 microsatellites is low ($G_{ST} < 0.04$)
367 among the 8 Mediterranean shore crab populations (Figure 5D). Nevertheless, G_{ST} and H_S
368 estimates are highly negatively correlated, with a correlation coefficient of -0.80 and a small
369 p value (0.010). It is likely that mutations have substantially impacted on the G_{ST} estimates
370 from these microsatellites, and thus the underlying population differentiation due to
371 demography may well be underestimated by these microsatellites.

372 The 17 microsatellites in blacktip reef sharks are highly variable in diversity, with the
373 number of observed alleles varying from 4 to 48 and the H_S varying from 0.15 to 0.89. The
374 G_{ST} values among the 15 populations estimated from the 17 loci are also highly variable,
375 from 0.04 to 0.41 (Figure 5E). The 3 loci showing deviation from Hardy-Weinberg
376 equilibrium are apparently not outliers in terms of both diversity and differentiation. The
377 single locus G_{ST} and H_S estimates are highly negatively correlated, with a correlation
378 coefficient of -0.890 ($p=0.000 \times 10^{-6}$) and -0.913 ($p=0.000 \times 10^{-6}$) for the entire set of 17 loci
379 and the subset of 14 loci respectively. In this system, mutations are highly likely to have
380 reduced the differentiation of the microsatellites; the underlying population differentiation
381 due to drift and migration should be higher than the average G_{ST} value calculated from these
382 microsatellites.

383 The differentiation measured by G_{ST} at each of the 17 microsatellites is low among the
384 10 copper rockfish populations (Figure 5F). Except for locus Sra11-103 which has a $G_{ST} =$
385 0.09, single locus G_{ST} values are below 0.05. The overall mean G_{ST} across loci is 0.027, very
386 close to the F_{ST} value 0.031 obtained by Dick *et al.* (2014). Single locus G_{ST} and H_S estimates
387 are not correlated, with a correlation coefficient of 0.011 and a p value of 0.649. It can be
388 concluded confidently that mutations have no impact on these G_{ST} estimates, and all markers,
389 regardless of polymorphisms, should have the same expected differentiation which is
390 equivalent to the population differentiation. The average G_{ST} across loci, 0.027, should be an
391 unbiased estimate of the population differentiation due to demography.

392 **Discussion**

393 The claim that F_{ST} and G_{ST} are dependent on marker H_S and underestimate population
394 differentiation when calculated from highly polymorphic (i.e. high H_S) markers (e.g.

395 Nagylaki 1998; Hedrick 2005; Jost 2008) can be misleading. It has led to the conclusion that
 396 these traditional statistics should be either “corrected” for H_S (e.g. Hedrick 2005) or replaced
 397 by new statistics such as D (Jost 2008). The claim creates lots of confusions, as if F_{ST} and G_{ST}
 398 should be independent of H_S to be correct measures of differentiation. As Wright (1978, p.82)
 399 explicitly stated, however, F_{ST} (the same for G_{ST}) measures “the amount of differentiation
 400 among subpopulations, relative to the limiting amount under complete fixation”. Complete
 401 fixation means each subpopulation is fixed with an allele (i.e. all individuals in a
 402 subpopulation have the same homozygous genotype), which is not necessary to be unique
 403 among subpopulations. Fixation results in $H_S=0$, and the maximal differentiation of $F_{ST}=1$ is
 404 achieved only at $H_S=0$. For this reason, Wright (1951) also called his F_{ST} a fixation index,
 405 among other fixation indices of F_{IS} and F_{IT} . The quantity H_S measures the *absolute* distance
 406 from complete fixation (i.e. $H_S=0$), and naturally constrains F_{ST} , which measures the *relative*
 407 (to total diversity H_T) or standardized distance from complete fixation. The definition of
 408 $G_{ST} = 1 - H_S/H_T$ (Nei 1973) makes the functional relationship between absolute (i.e. H_S)
 409 and relative (i.e. G_{ST}) differentiations explicit. Therefore, both F_{ST} and G_{ST} legitimately
 410 depend on, or more precisely, are constrained by H_S . This relationship is true both
 411 mathematically and biologically, and does not inherently cause F_{ST} and G_{ST} to underestimate
 412 differentiation for markers with high H_S .

413 More precisely, F_{ST} and G_{ST} become marker dependent and underestimate population
 414 differentiation only when migration rate is lower than mutation rate. Otherwise, they provide
 415 accurate estimates of population differentiation regardless of marker H_S . In a population with
 416 low migration rates (i.e. $m < u$), a marker with a higher u is expected to have a higher H_S (or
 417 absolute differentiation) and a correspondingly lower G_{ST} (or relative differentiation) in both
 418 equilibrium and many non-equilibrium conditions (Whitlock 2011; this study). It should be
 419 emphasized that a high u does not necessarily lead to a high H_S , and *vice versa*. This is
 420 because it is the quantity uN rather than u that determines H_S . A marker with a small u in a
 421 population with a large N can still harbour a high H_S , and a marker with a large u in a
 422 population with a small N can still have a low H_S . The statement that microsatellites, because
 423 of their high allelic polymorphisms and high H_S , must always underestimate differentiation is
 424 imprecise. Such markers show less differentiation than less polymorphic markers (e.g. SNPs)
 425 only when migration is weak ($m < u$), as illustrated by Figures 1 and 2.

426 This study reveals that whenever $m < u$ and thus mutations have a substantial impact,
 427 single locus G_{ST} values decrease almost linearly with single locus H_S . This is true in both

428 equilibrium (Figure 1) and non-equilibrium populations, as verified by simulations under
429 different migration and mutation models (Figure 3). It is not surprising that the pattern
430 observed under the ideal island migration model and the infinite allele mutation model
431 applies to other migration and mutation models, because G_{ST} and F_{ST} are defined as
432 descriptive statistics without any predefined demographic and mutation models. Mutations
433 act to increase genetic diversity (H_S and H_T) and thus to decrease differentiation among
434 subpopulations, no matter they occur in the finite or infinite allele model or in the stepwise
435 mutation model (Wright 1943). Migrations, in contrast, tend to redistribute genetic diversity
436 evenly among subpopulations. Thereby they tend to reduce the difference between H_S and H_T
437 and thus to reduce G_{ST} , no matter they occur in the island model, stepping stone model or the
438 isolation-by-distance model.

439 The simulations confirm that a correlation analysis between single locus G_{ST} and H_S
440 estimates can be used to detect the mutational effects on differentiation. Under typical
441 sampling intensities, the analysis has sufficient power to identify the mutational effect when
442 it is present, and it does not falsely detect the mutational effect when it is absent (Figure 4),
443 when the significance level is chosen as $p=0.001$. A higher significance p value (say, 0.05 or
444 0.01) leads to higher powers, but also higher false detect rates. Under the finite island and
445 infinite allele models (first row in Figure 4), for example, the power (when $m=0.001$) and
446 false detection rate (when $m=0.01$) increase to 86.7% and 11.8% respectively when $p=0.01$,
447 and to 90.7% and 30.0% respectively when $p=0.05$. A good balance between type I and II
448 errors is achieved at $p=0.001$, which leads to a false detection rate being always below 7%
449 irrespective of the widely varying sampling intensities of the number of subpopulations, the
450 number of individuals per subpopulation, and the number of loci and polymorphisms (Figure
451 4).

452 Two out of the five empirical microsatellite datasets (Figures 5A, 5E) show strong
453 evidence (a high negative r_{GH} value and a small p value) that mutations have reduced G_{ST}
454 estimated from microsatellites, two datasets (Figures 5C, 5D) indicate a similar trend with
455 higher uncertainties, and the remaining dataset (Figure 5F) shows no detectable effect of
456 mutations on G_{ST} . It is noticeable that the copper rockfish populations (Figure 5F) have high
457 and widely variable H_S values across the 17 microsatellites, the highest H_S being 0.936. These
458 H_S values are similar to those of the microsatellites in Atlantic salmon populations (Figure 5A)
459 and the blacktip reef shark populations (Figure 5E). Yet, contrasting patterns of G_{ST} and H_S
460 were observed among the three species. This again verifies the theory and simulation based

461 conclusion that a high H_S does not necessarily lead to marker dependent G_{ST} , and does not
462 necessarily result in underestimation of population differentiation. In situations where the
463 correlation between G_{ST} and H_S has a high uncertainty (e.g. Figure 5C), collection of more
464 data (by sampling more subpopulations, loci, and individuals) may confirm or reject the
465 hypothesis that G_{ST} in a study system is affected by H_S or mutations. In contrast, the analysis
466 of a big SNP dataset (Figure 5B) does not detect any mutational effect. The correlation
467 between single locus G_{ST} and H_S values, 0.044, is small and positive, and clearly indicates no
468 mutational effects on G_{ST} . The results are understandable because the u for SNPs can be
469 several orders smaller than that for microsatellites, and as a result is more likely to be smaller
470 than migration rate m .

471 The five empirical microsatellite datasets were taken from the most recent literature at
472 random with regard to the relationship between G_{ST} and H_S , which was revealed only after the
473 correlation analyses. If this small sample of datasets represents the reality, then we may
474 conclude that underestimation of differentiation by microsatellites could be a common
475 problem (Hedrick 1999, 2005; Jost 2008). A meta-analysis of many more microsatellite
476 datasets as exemplified in this study is required for a solid conclusion. However, while
477 microsatellites do underestimate differentiation in some (or many) situations, they can also
478 yield unbiased estimates in situations where migration is high as shown for the copper
479 rockfish populations (Figure 5F). The assertion that all microsatellites of high H_S
480 underestimate differentiation and therefore all G_{ST} estimates should be standardized (Hedrick
481 2005) or abandoned and replaced by new differentiation statistics (Jost 2008) is unjustified.
482 In addition to the problems shown before (Ryman & Leimar 2009; Whitlock 2011; Wang
483 2012), these new statistics are also marker diversity dependent as shown below.

484 It is notable that several authors have conducted a meta-analysis of the relationship
485 between G_{ST} and H_S across species/populations (Heller & Siegismund 2009; Meirmans &
486 Hedrick 2011). They found that the estimated G_{ST} is always smaller than the maximum value
487 of $1 - H_S$, as expected, and shows a weak negative correlation with H_S . It should be pointed
488 out that the correlation analysis proposed in my study is fundamentally different from that in
489 these meta-analyses. In the latter, the correlation is at the species level, where G_{ST} and H_S are
490 average values across loci for each species. Because different species may have experienced
491 different evolutionary forces and demography such that their G_{ST} values differ, it is unclear
492 what the hypothesis these meta-analyses are trying to prove or disapprove, except for the
493 functional relationship $G_{ST} < 1 - H_S$ which should however always be true from the definition

494 of G_{ST} . The presence of a negative correlation between G_{ST} and H_S does not prove that G_{ST} is
 495 underestimated and is marker dependent because of mutational effects. The absence of the
 496 correlation does not prove that mutations have negligible effects and G_{ST} is unbiased and
 497 marker independent. In my study, the correlation is between single locus values of G_{ST} and
 498 H_S within a species (population). The hypothesis, clearly defined and supported by theory and
 499 simulations, is that G_{ST} values should be similar across markers of different H_S if mutations
 500 are unimportant (when $u < m$), resulting in an r_{GH} not different from 0. Otherwise (i.e. $u > m$),
 501 G_{ST} values should decrease with markers showing an increasing H_S , resulting in a highly
 502 negative correlation between G_{ST} and H_S .

503 G_{ST} calculated from a locus measures the genetic differentiation among
 504 subpopulations at the locus due to the combined effect of all evolutionary forces (Nei 1973).
 505 Selection directly influences F_{ST} and G_{ST} , as Wright (1943) illustrated with several different
 506 types of selection. In principle, a negative correlation between H_S and G_{ST} can also be
 507 generated for markers closely linked with a locus under strong selection for spatially different
 508 alleles (which causes a decrease in H_S and an increase in G_{ST}) or/and for spatially different
 509 allele combinations (which causes an increase in H_S and a decrease in G_{ST}). Although my
 510 correlation analysis assumes the absence of selection, it should be robust in most applications.
 511 First, frequently only a few microsatellites (<30) are used in calculating F_{ST} or G_{ST} , and the
 512 chance of any of them being under selection or being linked to loci under selection strong
 513 enough (compared with other evolutionary forces) for detection is slim. Second, with
 514 genomic dense markers such as SNPs, it is highly likely that a small fraction of the loci are
 515 under strong selection. The correlation analysis should however still be robust because the
 516 vast majority of loci are neutral and a few selected loci should not affect the overall
 517 relationship between H_S and G_{ST} .

518 This study focusses on the widely applied differentiation statistic G_{ST} (Nei 1973).
 519 Other differentiation statistics or estimators such as θ (Weir & Cockerham 1984), D (Jost
 520 2008) and G'_{ST} (Hedrick 2005) could also be affected by mutations and yield marker (H_S)
 521 dependent estimates. All these statistics measure differentiation at marker loci due to the
 522 collective actions of all evolutionary forces, including mutations. When mutations are
 523 important (i.e. $u > m$), therefore, differentiation estimates are expected to be different among
 524 loci. Some statistics, like D which is claimed to outperform G_{ST} for highly polymorphic
 525 markers (Jost 2008), are even more problematic and produce marker dependent
 526 differentiation estimates even when mutation rate is small relative to migration rate. For the

527 data simulated in finite island and infinite allele models, finite island and stepwise mutation
 528 models, and stepping stone and stepwise mutation models shown in Figure 3, for example,
 529 the correlation coefficient between D and H_S , r_{DH} , is 0.43, 0.30, and 0.22 respectively when
 530 $m=0.001$, and is 0.71, 0.24 and 0.26 respectively when $m=0.01$. The correlation is always
 531 positive and substantially high, even in the situation where mutation is very weak relative to
 532 migration and G_{ST} is uncorrelated with H_S . Similarly highly positive r_{DH} values are obtained
 533 for all of the empirical datasets. For the Atlantic salmon SNP dataset, r_{DH} is 0.73 while r_{GH} is
 534 only 0.04. This means D always increases with H_S , even for markers with low mutation rate
 535 (e.g. SNPs) and low diversity, and for a population with a high migration rate.

536 Slatkin's (1995) R_{ST} provides unbiased estimates of population differentiation
 537 regardless of the mutation rates or diversity of markers. A mutation does not erase the
 538 evolutionary history of a gene when it occurs in some models such as the stepwise model.
 539 Mutations occurring in these models are accommodated by R_{ST} , which therefore measures
 540 differentiation purely due to population demography (m and N). Unfortunately, however, R_{ST}
 541 is sensitive to violations of the assumed mutation models and have a higher sampling
 542 variance than G_{ST} (Balloux & Lugon-Moulin 2002). Unless many (say in the hundreds)
 543 markers are used, R_{ST} may have a lower accuracy than G_{ST} .

544 What are the uses of a correlation analysis on G_{ST} and H_S ? What we are usually
 545 interested are population level forces such as migration (or isolation) and drift, which have
 546 roughly the same effect on all loci in the genome, and population differentiation, which
 547 depends on population level forces and is estimated by all loci mainly controlled by
 548 population level forces. G_{ST} always faithfully reflects the differentiation at the marker loci, no
 549 matter the loci are governed primarily by population demography (m and N) or locus specific
 550 forces such as selection and mutation. Marker G_{ST} provides an unbiased and good estimate of
 551 population differentiation only when these markers are not significantly affected by locus
 552 specific forces. The correlation analysis essentially tests whether different markers give
 553 replicated or different estimates of G_{ST} , or whether or not population level forces are much
 554 more important than locus specific forces in shaping the marker diversity and distribution. A
 555 highly negative correlation between G_{ST} and H_S values indicates that 1) the migration rate
 556 must be low, lower than the mutation rate; 2) the marker G_{ST} may well underestimate
 557 population differentiation; 3) another set of markers with lower (higher) polymorphisms may
 558 well yield a higher (lower) estimate of G_{ST} ; 4) the marker G_{ST} should be used cautiously in
 559 comparisons across species, studies and sets of loci. If the correlation between G_{ST} and H_S

560 values among loci is small and non-significant, then these single locus G_{ST} estimates should
 561 be marker (diversity) independent and can be averaged to provide a good estimate of
 562 population differentiation.

563 A computer program, **CoDiDi** (**C**orrelation between **D**iversity and **D**ifferentiation), is
 564 written to calculate single locus G_{ST} and H_S values, to test whether a single locus G_{ST} value is
 565 significantly different from 0 or not by permutations, and to calculate and test the
 566 significance of the correlation between G_{ST} and H_S . The correlation analyses of all of the
 567 simulated and empirical data presented in this study were conducted by this program, freely
 568 available from the website: <http://www.zsl.org/science/software/CoDiDi>.

569

570 **Acknowledgments**

571 I thank PW Hedrick, PG Meirmans, N Ryman, Robin Waples, MC Whitlock and an anonymous referee for
 572 valuable comments on earlier versions of this manuscript.

573

574 **References**

- 575 Balloux F, Lugon-Moulin N (2002) The estimation of population differentiation with
 576 microsatellite markers. *Molecular Ecology*, **11**, 155-165.
- 577 Balloux F, Brunner H, Lugon-Moulin N, Hausser J, Goudet J (2000) Microsatellites can be
 578 misleading: an empirical and simulation study. *Evolution*, **54**, 1414–1422.
- 579 Carreras-Carbonell J, Macpherson E, Pascual M (2006) Population structure within and
 580 between subspecies of the Mediterranean triplefin fish *Tripterygion delaisi* revealed by
 581 highly polymorphic microsatellite loci. *Molecular Ecology*, **15**, 3527–3539.
- 582 Dick S, Shurin JB, Taylor EB (2014) Replicate divergence between and within sounds in a
 583 marine fish: the copper rockfish (*Sebastes caurinus*). *Molecular Ecology*, **23**, 575-590.
- 584 Hedrick PW (1999) Perspective: highly variable loci and their interpretation in evolution and
 585 conservation. *Evolution*, **53**, 313–318.
- 586 Hedrick PW (2005). A standardized genetic differentiation measure. *Evolution*, **59**, 1633–
 587 1638.
- 588 Heller R, Siegismund H (2009) Relationship between three measures of genetic
 589 differentiation G_{ST} , D_{EST} and G'_{ST} : how wrong have we been? *Molecular Ecology*, **18**,
 590 2080–2083.

- 591 Jin L, Chakraborty R (1995) Population structure, stepwise mutation, heterozygote deficiency
592 and their implications in DNA forensics. *Heredity*, **74**, 274-285.
- 593 Jost L (2008) G_{ST} and its relatives do not measure differentiation. *Molecular Ecology*, **17**,
594 4015–4026.
- 595 Kimura M, Crow JF (1964) The number of alleles that can be maintained in a finite
596 population. *Genetics*, **49**, 725-738.
- 597 Kimura M, Weiss G (1964) The stepping-stone model of population structure and the
598 decrease of genetic correlation with distance. *Genetics*, **49**, 561-576.
- 599 Li W-H (1976) Effect of migration on genetic distance. *American Naturalist*, **110**, 841–847.
- 600 Meirmans PG, Hedrick PW (2011) Assessing population structure: F_{ST} and related measures.
601 *Molecular Ecology Resources*, **11**, 5–18.
- 602 Moore JS, Bourret V, Dionne M *et al.* (2014) Conservation genomics of anadromous Atlantic
603 salmon across its North American range: outlier loci identify the same patterns of
604 population structure as neutral loci. *Molecular Ecology*, **23**, 5680-5697.
- 605 Nagylaki T (1998) Fixation indices in subdivided populations. *Genetics*, **148**, 1325–1332.
- 606 Nei M (1973) Analysis of gene diversity in subdivided populations. *Proceedings of the*
607 *National Academy of Sciences of the United States of America*, **70**, 3321–3323.
- 608 Nei M (1975) *Molecular Population Genetics and Evolution*. North-Holland, Amsterdam,
609 Netherlands.
- 610 Nei M (1977) F -statistics and analysis of gene diversity in subdivided populations. *Annals of*
611 *Human Genetics*, **41**, 225-233.
- 612 Nei M, Chesser R (1983) Estimation of fixation indices and gene diversities. *Annals of*
613 *Human Genetics*, **47**, 253–259.
- 614 Ohta T, Kimura M (1973) A model of mutation appropriate to estimate the number of
615 electrophoretically detectable alleles in a finite population. *Genetical Research*, **22**, 201-
616 204.
- 617 Portnoy DS, Hollenbeck CM, Belcher CN *et al.* (2014) Contemporary population structure
618 and post-glacial genetic demography in a migratory marine species, the blacknose shark,
619 *Carcharhinus acronotus*. *Molecular Ecology*, **23**, 5480-5495.
- 620 Pritchard JK, Stephens M, Donnelly P (2000) Inference of population structure using
621 multilocus genotype data. *Genetics*, **155**, 945-959.
- 622 Ryman N, Leimar O (2008) Effect of mutation in genetic differentiation among
623 nonequilibrium populations. *Evolution*, **62**, 2250–2259.

- 624 Ryman N, Leimar O (2009) G_{ST} is still a useful measure of genetic differentiation—a
625 comment on Jost's D . *Molecular Ecology*, **18**, 2084–2087.
- 626 Sanetra M, Crozier R (2003) Patterns of population subdivision and gene flow in the ant
627 *Nothomyrmecia macrops* reflected in microsatellite and mitochondrial DNA markers.
628 *Molecular Ecology*, **12**, 2281–2295.
- 629 Schiavina M, Marino IAM, Zane L, Melià P (2014) Matching oceanography and genetics at
630 the basin scale. Seascape connectivity of the Mediterranean shore crab in the Adriatic
631 Sea. *Molecular Ecology*, **23**, 5496–5507.
- 632 Slatkin M (1995) A measure of population subdivision based on microsatellite allele
633 frequencies. *Genetics*, **139**, 457–462.
- 634 Takahata N, Nei M (1984) F_{ST} and G_{ST} statistics in the finite island model. *Genetics*, **107**,
635 501–504.
- 636 Vignaud TM, Mourier J, Maynard JA *et al.* (2014). Blacktip reef sharks, *Carcharhinus*
637 *melanopterus*, have high genetic structure and varying demographic histories in their
638 Indo-Pacific range. *Molecular Ecology*, **23**, 5193–5207.
- 639 Wang J (2012) On the measurements of genetic differentiation among populations. *Genetics*
640 *Research*, **94**, 275–289.
- 641 Wang J, Caballero A (1999) Developments in predicting the effective size of subdivided
642 populations. *Heredity*, **82**, 212–226.
- 643 Weir BS, Cockerham CC (1984) Estimating F -statistics for the analysis of population
644 structure. *Evolution*, **38**, 1358–1370.
- 645 Whitlock MC (2011) G_{ST} and D do not replace F_{ST} . *Molecular Ecology*, **20**, 1083–1091.
- 646 Wright S (1931) Evolution in Mendelian populations. *Genetics*, **16**, 97–159.
- 647 Wright S (1943) Isolation by distance. *Genetics*, **28**, 114–138.
- 648 Wright S (1951) The genetical structure of populations. *Annals of Eugenics*, **15**, 323–354.
- 649 Wright S (1969) *Evolution and the Genetics of Populations, Vol. II. The Theory of Gene*
650 *Frequencies*. University of Chicago Press, Chicago.
- 651 Wright S (1978) *Evolution and the Genetics of Populations, Vol. IV. Variability Within and*
652 *Among Natural Populations*. University of Chicago Press, Chicago.
- 653
- 654
-

655 J. Wang is interested in developing population genetics models and methods of analysis of
656 empirical data to address issues in evolutionary and conservation biology.
657

658

659 **Data accessibility**

660 The computer program for simulating genotype data under different migration and mutation
661 models, and for estimating H_S , G_{ST} and their correlation: Dryad DOI: 10.5061/dryad.733s9.

662 The 6 empirical datasets were retrieved from Dryad with DOIs:
663 <http://dx.doi.org/10.5061/dryad.sb601>; <http://dx.doi.org/10.5061/dryad.vv277>;
664 <http://dx.doi.org/10.5061/dryad.r0d1q>; <http://dx.doi.org/10.5061/dryad.th4h5>;
665 <http://dx.doi.org/10.5061/dryad.s489b>

666 The input files of the 6 empirical datasets for **CoDiDi** analysis: Dryad DOI:
667 10.5061/dryad.733s9.

668

669

Table 1 Parameter ranges in simulations

Migration model	Mutation Model	t	m	u	M	R	L
FIM, SSM	IAM, SWM, FAM	200, ∞	0.01,0.001	$10^{-5}\sim 10^{-3}$	10, 20, 40, 80, 160	2, 3, 4, 6, 8, 10, 12	5, 10, 15, 20, 30

670 The size (N) and number (s) of subpopulations are fixed at 250 (or 1000) and 20, respectively.

671 The finite island model (FIM) and circular stepping stone model (SSM) for migrations are

672 considered for neutral loci under infinite allele model (IAM), stepwise model (SWM) or

673 finite allele model (FAM) for mutations. For FAM, 2 alleles are considered to mimic SNPs.

674 Symbols t , m , u , M , R , L represent number of generations when sampling occurs, migration

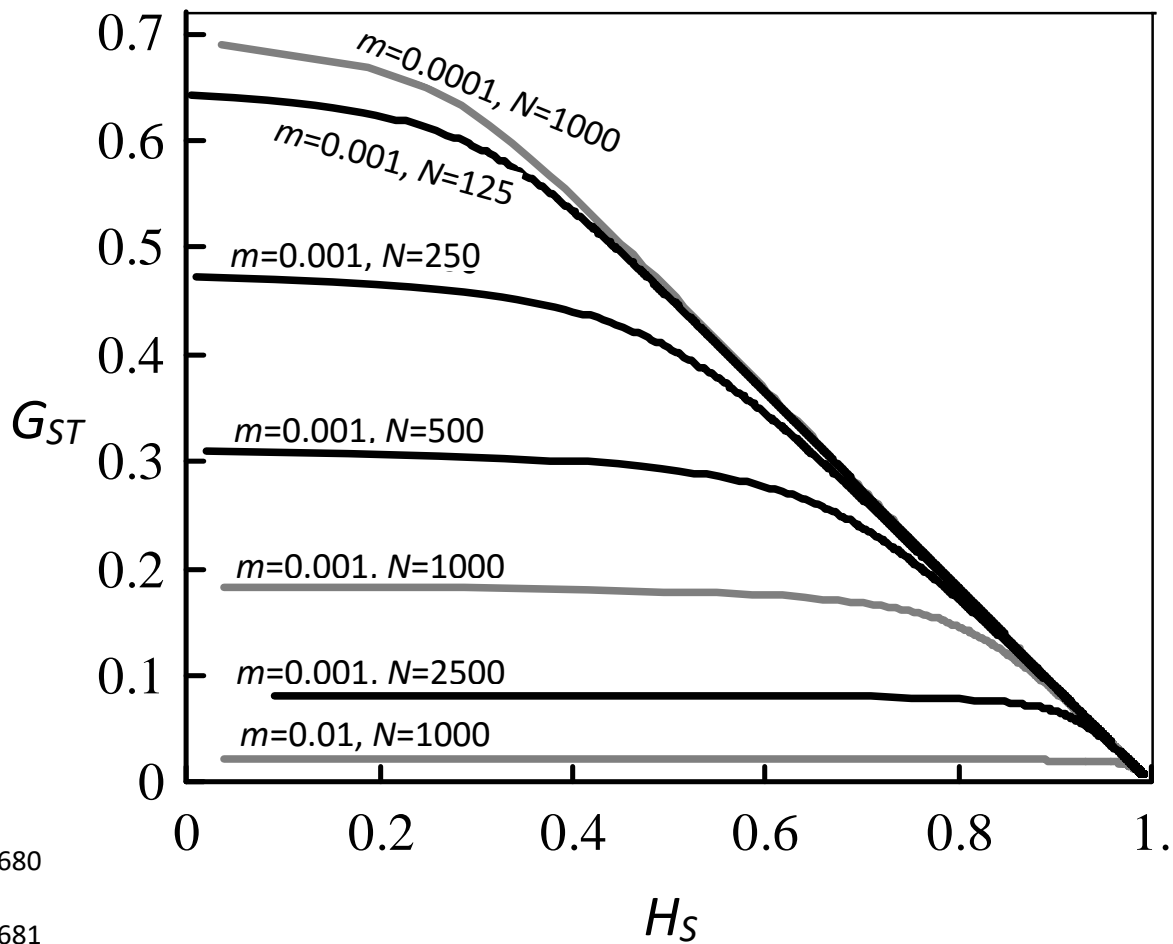
675 rate, mutation rate, number of individuals sampled from a subpopulation, number of sampled

676 subpopulations, and number of sampled loci, where $t=\infty$ indicates a population at mutation-

677 drift-migration equilibrium.

678

679



680

681

682

683

684

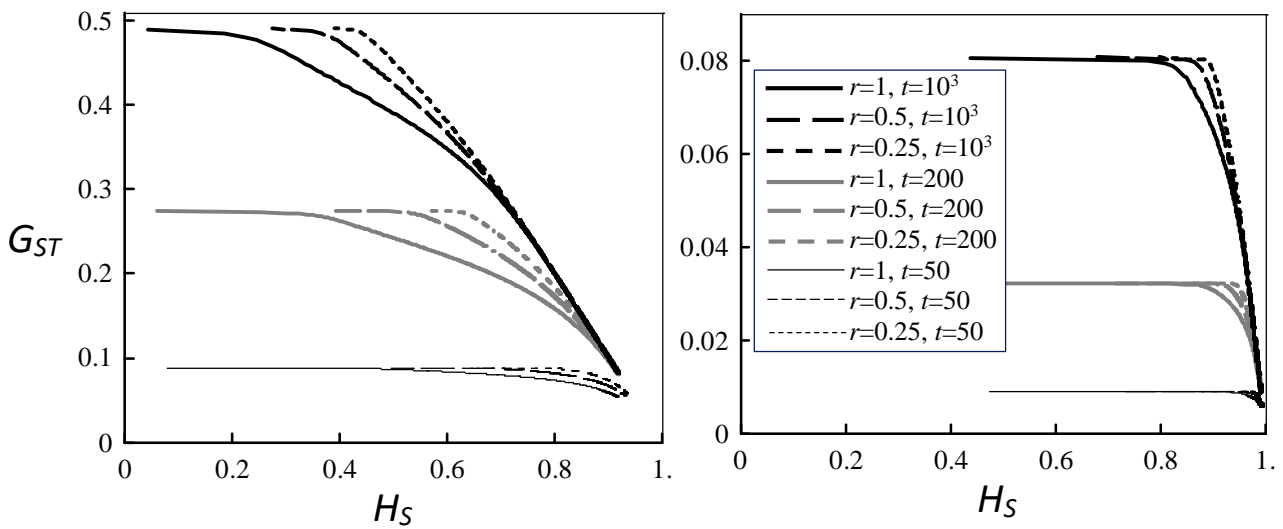
685

686

687

688 **Fig. 1** G_{ST} as a function of H_S in equilibrium populations. The G_{ST} (y axis) and H_S (x axis)
 689 values for a population in a finite island model with $s=10$ subpopulations at mutation-drift-
 690 migration equilibrium were calculated for various parameter values of subpopulation size (N),
 691 migration rate (m), and mutation rate (u), where u ranges from 10^{-6} (left side of x axis) to 10^{-2}
 692 (right side of x axis).

693



694

695

696

697

698

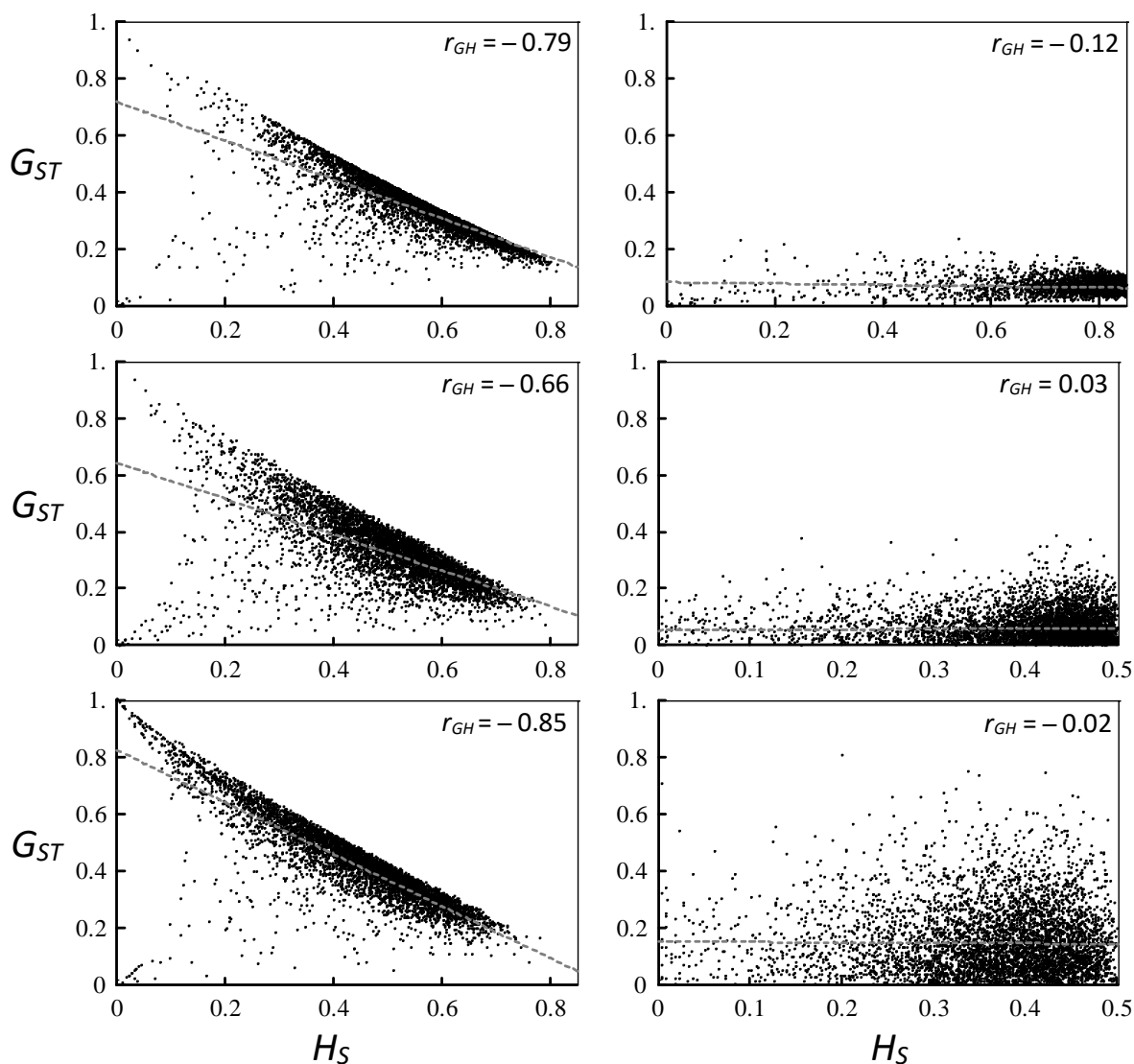
699

700

701

702 **Fig. 2** G_{ST} as a function of H_S in non-equilibrium populations. The G_{ST} (y axis) values are
 703 plotted against H_S (x axis) values at different generations ($t=50, 200, 1000$) for a population
 704 in a finite island model with $s=10$ subpopulations, assuming parameter values of $N=250$ (left
 705 panel) or 1000 (right panel), $m=0.001$, and a variable u ranging from 10^{-6} (left side of x axis)
 706 to 10^{-2} (right side of x axis). The initial probability of gene identity is assumed to be $rJ_{0(\infty)}$,
 707 where $r=1, 0.5$ and 0.25 and $J_{0(\infty)}$ is the equilibrium value of J_0 given parameters N, m, u, s .

708



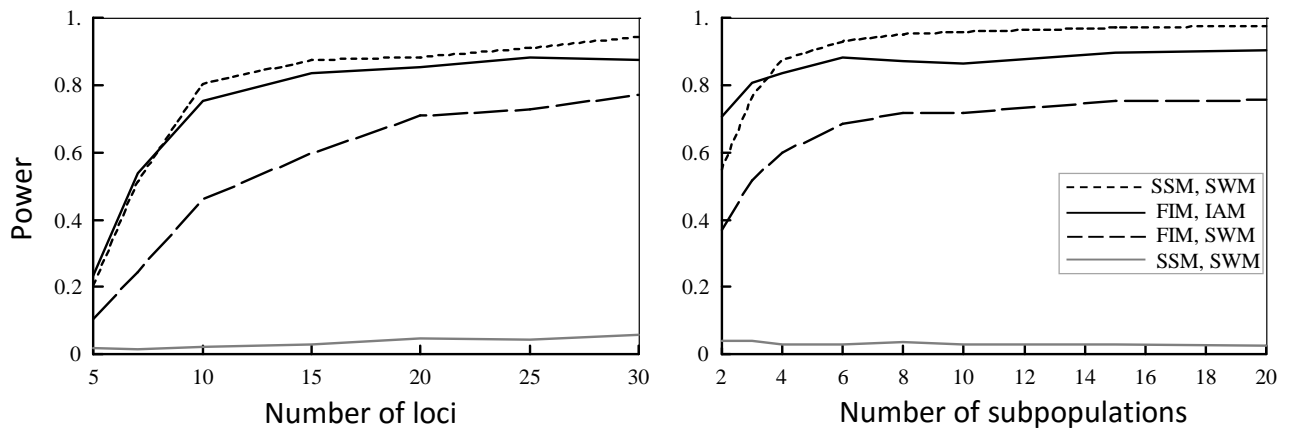
709

710

711

712 **Fig. 3** Scatter graphs of G_{ST} (y axis) and H_S (x axis) estimates in mutation-drift-migration
 713 equilibrium populations. The population parameters are $N=250$, $s=20$, u is taken at random
 714 from a uniform distribution in the range $[10^{-5}, 10^{-3}]$, and migration rate is either $m=0.001$ (left
 715 column) or $m=0.01$ (right column). The population is assumed to follow the finite island and
 716 infinite allele models (first row), finite island and stepwise mutation models (second row), or
 717 stepping stone and stepwise mutation models (third row). For each graph, 5000 replicate
 718 simulated datasets (loci) were generated to estimate G_{ST} and H_S , using $R=4$ (out of $s=20$)
 719 randomly sampled subpopulations and $M=50$ (out of $N=250$ or 1000) randomly sampled
 720 individuals per subpopulation. The correlation between the G_{ST} and H_S estimates for each
 721 graph is shown at the right corner of the graph.

722

723
724

725

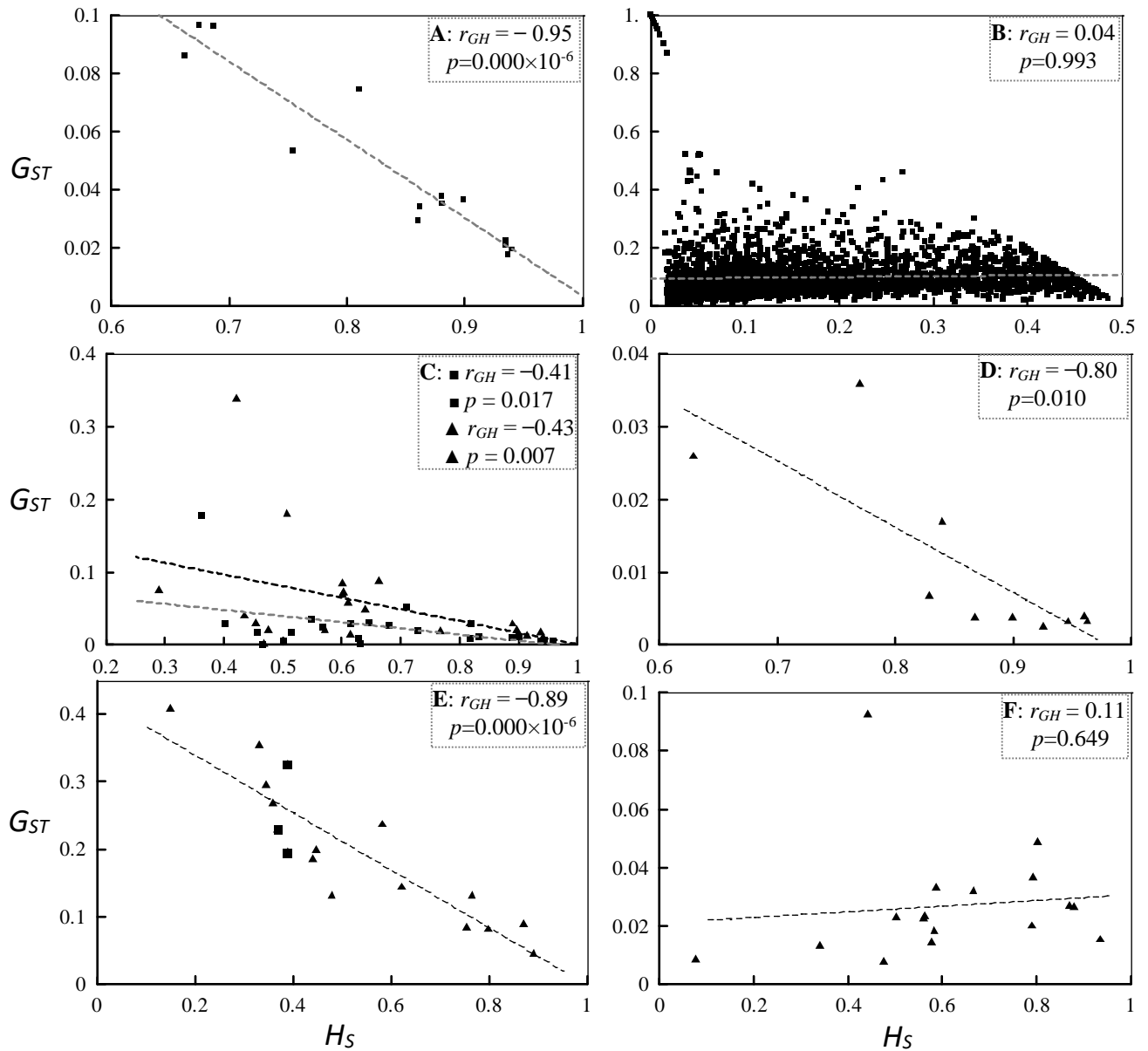
726

727

728

729 **Fig. 4** Power of correlation analysis of G_{ST} and H_S estimates in mutation-drift-migration
 730 equilibrium populations. The population parameters are $N=250$, $s=20$, and u is taken at
 731 random from a uniform distribution in the range $[10^{-5}, 10^{-3}]$. The numbers of sampled
 732 subpopulations and loci are 4 and variable for the left panel, or variable and 15 for the right
 733 panel. Migration rate is either $m=0.001$ (black continuous, black broken and black dotted
 734 lines) or $m=0.01$ (grey continuous lines). The population is assumed to follow the finite
 735 island model (FIM) and infinite allele model (IAM), finite island model and stepwise
 736 mutation model (SWM), or stepping stone model (SSM) and stepwise mutation model. For
 737 each parameter combination, the proportion of 1000 replicate datasets in which the
 738 correlation coefficient between G_{ST} and H_S , estimated using 40 individuals per sampled
 739 subpopulation, is statistically significant at $p<0.001$ is plotted (on y axis) as a function of the
 740 number of sampled loci (left panel) or the number of sampled subpopulations (right panel)
 741 (on x axis). The black lines show the power in detecting mutational effects on G_{ST} when such
 742 effects exist (i.e. when migrations are weak relative to mutations, $m=0.001$), and the grey
 743 lines show the false detection rates when mutational effects are absent (i.e. when migrations
 744 are strong relative to mutations, $m=0.01$).

745



746
747

748

749

750

751

752

753 **Fig. 5** The relationship between single locus G_{ST} and H_S estimates in empirical datasets. The
754 correlation coefficient between G_{ST} and H_S and the p value for each dataset are shown at the
755 top right corner of each graph, and the grey dotted lines show the fitted regression of G_{ST} on

756 H_S . Graphs A and B show the results for the 15 microsatellites and 3129 SNPs respectively in
757 North American Atlantic salmon populations. Graph C shows the results for the 23
758 microsatellites in the blacknose shark populations, where each triangle and each square
759 shows the pair of G_{ST} and H_S values estimated from a single marker in the 2- and 10-
760 population models, respectively. Graph D shows the results for the 10 microsatellites in eight
761 Mediterranean shore crab populations. Graph E shows the results for the 17 microsatellites in
762 15 blacktip reef shark populations, where each triangle and each square represents a single
763 marker without and with deviation from Hardy-Weinberg equilibrium. Graph F shows the
764 results for the 17 microsatellites in 10 copper rockfish populations.

765